Mem. S.A.It. Vol. 74, 367

Memorie della

Obscuration and reprocessing in the cosmic history of active galactic nuclei

G. Matt[1,⋆] C. Bongardo[2], V. Braito[2], M. Brusa[3], A. Caccianiga[4], F. La Franca[1], A. Marconi[5], and P. Marziani[2]

[1] Dipartimento di Fisica, Università degli Studi Roma Tre, Roma, Italy
[2] INAF, Osservatorio Astronomico di Padova, Padova, Italy
[3] INAF, Osservatorio Astronomico di Bologna, Bologna, Italy
[4] INAF, Osservatorio Astronomico di Brera, Milano, Italy
[5] INAF, Osservatorio Astrofisico di Arcetri, Firenze, Italy

Abstract. The Cofin 2000 project titled 'Obscuration and reprocessing in the cosmic history of AGN' aims to study the physical and morphologic characteristics of the obscuring material in active galactic nuclei (AGN), and the cosmic history of the obscured AGN, to be compared with the history of unobscured AGN and with that of star formation. The project is in progress; as it is still too early to make a synthesis of the results, we will instead discuss separately the status of several different lines of research.

Key words. surveys – galaxies: active – galaxies: quasars: general – galaxies: starburst

1. Introduction

The Cofin 2000 project titled 'Obscuration and reprocessing in the cosmic history of AGN' aims to study the physical and morphologic characteristics of the material which surrounds and often obscures active galactic nuclei (AGN); to take a census of the absorbed AGN, and study their cosmological evolution; to correlate the presence of absorption with other characteristics of the AGN; to estimate the amount of nuclear radiation absorbed and reprocessed in the infrared along the cosmic history of AGN, and compare it with that of stellar origin, with the related implications on the birth and growth of quasar and the connections with the history of star formation.

The project team includes five institutions: INAF/Arcetri Observatory (M. Salvati, R. Maiolino, A. Marconi, E. Oliva, G. Torricelli Ciamponi, plus P. Pietrini at the Astronomy Department, to mention staff members only), INAF/Bologna Observatory (A. Comastri, P. Ciliegi, M. Mignoli, G. Stirpe), INAF/Milano Observatory (T. Maccacaro, R. Della Ceca, A. Wolter), INAF/Padova Observatory (P. Marziani, P. Andreani, M. Calvani),

Send offprint requests to: G. Matt
⋆ On behalf of the whole team
Correspondence to: Dipartimento di Fisica, Università degli Studi Roma Tre, Via della Vasca navale 84, I-00146 Roma, Italy

Università Roma Tre, Physics Department (G. Matt, A. Altamore, F. La Franca, G. C. Perola, plus F. Fiore at INAF/Rome Observatory).

In the following, several different researches will be discussed separately, as it is still too early to make a synthesis of the results of the project, which of course is still in progress. Even if what will be described later do not exhaust all the topics studied, we believe it is a fair sample of the on–going activities.

To better understand what follows, it may be useful to introduce the so–called AGN Unification Model (Antonucci 1993), firstly proposed to explain the differences between type 1 and type 2 Seyfert galaxies. In this scenario, Seyfert 1s (in which both broad and narrow lines are visible in the optical spectrum) and Seyfert 2s (where only narrow lines are observed) are intrinsically the same. The nucleus (i.e. the black hole with the accretion disc and the broad-line regions) is surrounded by optically and geometrically thick matter, probably axisymmetric (usually called the 'torus'). If the line-of-sight does not intercept the torus, the nucleus is visible and the source is classified as type 1. Otherwise, only the narrow-line regions are visible and the source is classified as type 2. In this scenario, a one-to-one relation between optical type-1 and X-ray unobscured sources, and between type-2 and X-ray obscured sources, is expected. One of the main result of our project is that some of the researches described below are calling for a revision of the Unification Model.

2. Morphology and physical properties of the obscuring medium (contributed by G. Matt)

In recent years it has become clear that, at least in the local Universe, absorbed AGN outnumbers unabsorbed ones by a factor of a few; moreover, in at least half of sources, the absorbing material is very thick, with a Compton scattering optical depth exceeding unity (e.g. Risaliti et al 1999; Matt et al. 2000). These sources are called Compton–thick and are particularly interesting because, being the nucleus completely invisible at least below ∼10 keV, reflection components from circumnuclear matter may be best studied. For a recent review on X–ray obscured AGN, see Matt (2002).

On the basis of BeppoSAX and ASCA spectra, and using the CLOUDY photoionization code, we indeed tried to constrain the physical and geometrical properties of the circumnuclear regions in the two brightest Compton–thick sources, the Circinus Galaxy and NGC 1068 (Bianchi et al. 2001). The results are: for the Circinus Galaxy, one mildly ionized, optically thick reflector, to be identified with the torus and with an inner radius of a fraction of a parsec, is sufficient to explain most of the line and continuum spectra; for NGC 1068, instead, at least three different reflectors (one cold and optically thick, to be identified with the torus and with inner radius of a few parsecs; the other two optically thin and photoionized, one mildly the other highly ionized) are required. Recent Chandra and XMM–Newton grating observations (e.g. Sambruna et al. 2001; Kinkhabwala et al 2002) have refined but substantially confirmed these findings.

An interesting recent result is that a few obscured AGN appear as Compton–thick (i.e. with only reflection components visible) or Compton–thin (with the nuclear radiation directly visible) when observed at different epochs (Matt et al. 2003 and references therein). While a change in the column density of the absorber cannot be ruled out, it appears rather unlikely, as discussed in Matt et al. (2003). The best explanation seems to be a temporarily switching–off of the nuclear radiation, similarly to what happened to the Seyfert 1 galaxy NGC 4051 (Guainazzi et al. 1998). When the source is switched-off, only the reflection components (from matter out of the line–of–sight) remain visible. Because among the reflection components there is a Compton–thick neutral reflector, this implies the co-existence of

two different circumnuclear neutral regions, one to be identified with the torus, the other (the Compton–thin one) associated either with the host galaxy disc (Maiolino & Rieke 1995) or with dust lanes (Matt 2000), thus requiring a modification of the zeroth–order Unification Model.

3. The ELAIS survey (contributed by F. La Franca)

The ELAIS survey (Oliver et al. 2000) is a collaboration of 19 European institutes, aiming to build a catalogue of sources detected by ISO at 7, 15, and 90 μm, over an area of 12 sq. deg., down to fluxes two orders of magnitude lower than those of IRAS. The Italian group, in Bologna and at Roma Tre, is in charge of the southern area ELAIS-S1 of 4 sq. deg. The ELAIS-S1 region is one of the most important in the southern sky for this kind of observations as it corresponds to the minimum of cirrus emission in the IR.

Recently, a new analysis of the ISOCAM data at 15 μm has been completed. A total of 462 sources have been found down to 0.5 mJy (Lari et al. 2001). The analysis of the number-counts has been published by Gruppioni et al. (2002). The area has been covered at 1.4 GHz with the Australia Telescope, and in the B, R, I bands with the 2.2/WFI and 1.5/Danish telescopes at ESO. Thanks to several spectroscopic campaigns carried out at the 2dF at the Anglo Australian Telescope, at the 1.52/Danish, NTT e 3.6-m telescopes from ESO, it has been possible to identify more than 200 sources with $R < 20$: mainly starburst galaxies and AGN (La Franca et al., in preparation). The preliminary analyses have allowed to derive, for the first time, the evolution of AGN at 15μm and the contribution of AGN to the IR cosmic background (Matute et al. 2002). This contribution is about 15%, roughly in agreement with theoretical predictions (Granato et al. 1997; Fabian & Iwasawa 1999) based on the estimate of the contribution of obscured AGN to the cosmic XRB.

The final analysis in the next 12 months will allow a) a better estimate of the evolution of type 1 and 2 AGN, and b) an unbiased estimate of the star formation rate at low redshifts ($z \sim 0.3$). ELAIS-S1 has also been covered in the hard X-ray band by BeppoSAX: the relationship between mid-IR and hard X-ray emission for the type 1 AGN has been measured down to fluxes 100 times fainter than before (Alexander et al. 2001).

4. The HELLAS2XMM survey (contributed by M. Brusa)

In order to better understand the nature of the various components of the cosmic X–ray background we have started a program of multiwavelength follow–up observations of hard X–ray selected sources serendipitously discovered in 15 XMM–Newton fields over ~ 3 deg^2 (the HELLAS2XMM survey; Baldi et al. 2002).

We have limited our survey at 2–10 keV fluxes of the order of $\sim 10^{-14}$ erg cm^{-2} s^{-1} where a significant fraction of the XRB is resolved ($\sim 50 - 60\%$; see, e.g., Comastri 2001 for a review) and at the same time the process of optical identification is relatively easy. This strategy allows to cover a relatively large area of the sky and to fill the gap between previous shallow hard X–ray surveys (the BeppoSAX HELLAS survey, Fiore et al. 2001; the ASCA GIS survey, Cagnoni, della Ceca & Maccacaro 1998; the ASCA LSS and MSS Surveys, Akiyama et al. 2000) and recent deep Chandra (CDF–N, Brandt et al. 2001; CDF–S, Giacconi et al. 2002) and XMM–Newton (Lockman Hole, Hasingher et al. 2001) observations.

The 2–10 keV sample of the HELLAS2XMM survey consists of 495 sources, selected on the cleaned XMM-Newton images with an accurate detection algorithm developed by our group (Baldi et al. 2002). To date, we have performed an extensive optical follow–up program for the five HELLAS2XMM fields accessible

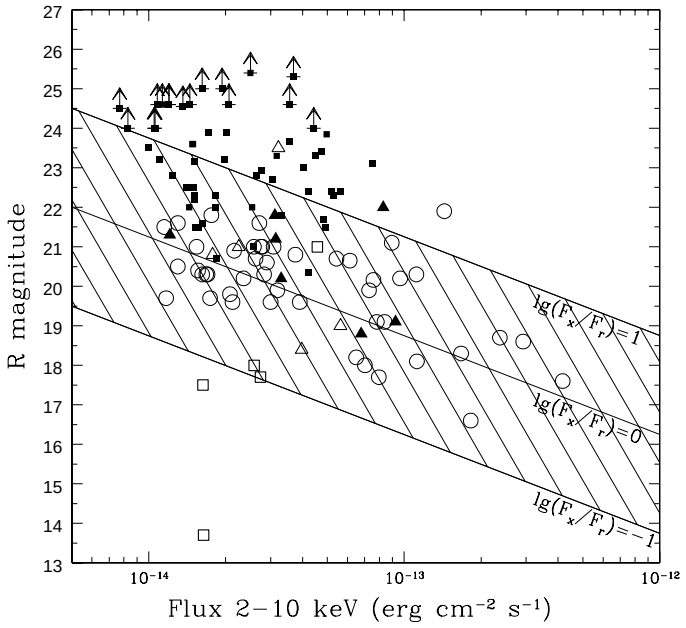

Fig. 1. R magnitude vs. hard X–ray flux for all the sources with optical coverage in the HELLAS2XMM sample. Empty circles = BL AGN; filled triangles = NL AGN; open triangles = ELG; open squares = XBONGs; filled squares and lower limts = unidentified objects. The solid lines represent the loci of constant X–ray–to–optical flux ratio (0.1, 1 and 10, respectively). See text for more details.

with both ESO (3.6-m telescope and VLT) and TNG telescopes (about one third of the entire sample). We have already obtained deep R–band ($R \approx 24 \div 25$) images for all the 127 sources in the subsample and good quality optical spectra at the ESO/3.6-m and TNG telescopes for almost all of the sources with $R < 22$ (72 objects, 'optically bright' population). Deep VLT/FORS1 spectroscopy of about 35 sources with $22 < R < 24$ has been performed during ESO period 70, while for the remaining ~ 20 objects with $R > 24$ we have obtained near–infrared imaging with ISAAC at VLT. The spectroscopic completeness of the present sample will thus be of $\sim 85\%$. The results of the optical identifications and spectroscopic classifications are summarized in Fig.1.

4.1. 'Optically bright' population

At the relatively bright 2–10 keV fluxes sampled by our survey, the identified objects are characterized by a wide spread in their optical properties (both in the continuum shape and the emission lines). The majority of the X–ray sources in the $R < 22$ sample turned out to be associated with optically unobscured, Broad–Line AGN (∼60%, open circles in Fig.1). However, the hard X–ray properties of a few high–redshift objects suggest the presence of a substantial column density in

their nuclei, confirming the BeppoSAX and ASCA discovery that 20–25% of type 1 AGN at $z > 0.5$ are very hard and thus possibly obscured (e.g. Fiore et al. 2001; Akyiama et al. 2000).

A significant fraction (∼20-25%) of hard X–ray sources has been identified with Narrow–Line AGN and Emission Line galaxies (filled and open triangles, respectively, in Fig.1) while a non negligible fraction (∼15%) is associated with sources that show indication of nuclear obscuration (e.g., hard X–ray colors) and peculiar optical properties such as the absence of activity (i.e. emission lines) in their spectra. These X–ray Bright Optically Normal Galaxies (XBONGs, open squares in Fig.1) have X–ray–to–optical flux ratios which are on average lower, but still consistent, with those of X–ray selected AGNs. However, their X–ray luminosity exceeds by more than one order of magnitude that predicted based on their optical luminosity for normal galaxies (Fabbiano, Kim & Trinchieri 1992) and it is similar to that of Seyfert galaxies. From a detailed multiwavelength analysis of the prototype of these objects (the so–called 'Fiore P3'), Comastri et al. (2002b) argued that an highly obscured, possibly Compton–thick AGN is responsible of the observed properties.

4.2. 'Optically Faint' population

About 45% of the hard X–ray selected sources are associated with faint optical counterparts ($R > 22$, filled squares and lower limits in Fig.1). Most of these sources are likely to be type 2 AGNs and a fraction of them could be high luminosity, type 2 QSOs. They show hard X–ray colors, suggesting that the active nucleus responsible of the hard X–ray emission suffers from substantial nuclear obscuration.

It is worth noting that about half of the sources among the 'optically faint' population are characterized by an X–ray–to–optical flux ratio (hereinafter X/O) greater than 10, more than one order of magnitude greater than the value expected for optically selected AGNs (Lehmann et al. 2001). This is a further indication that the majority, if not all, of the high X/O sources are powered by an X–ray active, optically obscured AGN. This hypothesis, confirmed by optical identification of an handful of sources that turned out to be Narrow Emission Line objects, will be definitively tested with the analysis of VLT/FORS1 data obtained as part of the optical identification program of faint X–ray sources. These 'extreme', unconventional X–ray sources represent ∼25% of the whole sample, and their fraction seems to be constant at lower flux limits in deep Chandra (∼26% in the CDFS, Giacconi et al. 2002; ∼22% in the CDFN, Barger et al. 2002) and XMM–Newton (∼30% in the Lockman Hole, Mainieri et al. 2002) observations. It is clear that shallow serendipitous surveys are better suited to select candidates for which optical identification and spectroscopy is feasible at 8m–class telescopes. Indeed, at the flux limit of deep Chandra surveys, similar objects would be fainter than $R \sim 27$ and they would probably remain undetected even in ultradeep optical observations. Alternatively, deep near–infrared imaging and spectroscopy could provide a powerful tool to uncover their nature.

5. Relic black holes and type 2 quasars (contributed by A. Marconi)

In this section, we follow the evolution of the Black Hole mass function in the assumption that mass accretion onto a massive BH is the powering mechanism of AGN activity. We will show that, with reasonable assumptions suggested by current knowledge, it is possible to reproduce the Black Hole mass function derived from local bulges. In particular we will show that the majority of the mass in relic Black Holes was produced during AGN activity and that the ratio between obscured and unobscured quasars is between 1 and 2, much lower than required by synthesis

models of the X-ray background. More details of can be found in Marconi & Salvati (2002).

To relate the BH mass function with the AGN luminosity function, we consider the continuity equation which regulates the time evolution of the BH mass function with the Small & Blandford (1992) formalism. If $N(M,t)$ is the BH mass function [$N(M,t)\mathrm{d}M$ is the number of BHs per unit comoving volume (Mpc^{-3}) at cosmic time t], the continuity equation can be written as:

$$\frac{\partial N}{\partial t} + \frac{\partial}{\partial M}\left(N < \dot{M}(M,t) >\right) = 0 \qquad (1)$$

where $< \dot{M}(M,t) >$ is the 'average' accretion rate. If AGNs are powered by accretion onto BHs, we can relate the AGN Luminosity Function $\phi(L,t)$ [$\phi(L,t)\mathrm{d}\ln L$ is the number of AGNs per unit comoving volume (Mpc^{-3}) at cosmic time t] to the BH mass function obtaining finally

$$\frac{\partial N(M,t)}{\partial t} = -\frac{c^2\lambda^2}{\varepsilon t_E^2}\left[\frac{\partial \phi(L,t)}{\partial L}\right]_{L=\lambda\frac{Mc^2}{t_E}} \qquad (2)$$

where all black holes are is emitting at a fraction λ of the Eddington rate (t_E is the Eddington time) with efficiency ε. This equation is integrated assuming that, at the starting redshift $z_\circ$, all Black Holes are active.

A fundamental ingredient is the AGN luminosity function (LF) expressed in terms of the total AGN luminosity, L. To describe high L objects, we consider the LF of optically selected quasars (OLF in the B band; Boyle et al. 2000). For low L objects we consider the LF of soft X-ray selected AGNs (XLF in 0.5-2 keV band; Gilli et al. 2001). Both LFs consider only type 1 (unobscured) AGNs. The total AGN LF is obtained by summing the two previous LFs assuming $L/L_{\mathrm{X}} = 30$, for low L objects, and $L/\nu_{\mathrm{B}}L_{\nu_{\mathrm{B}}} = 15$ as typical of quasars.

The local BH mass function is estimated from the local galaxy luminosity function as a consequence of the well known correlation between the BH mass and the luminosity of the host spheroid. To do this we follow the method by Salucci et al. (1999). The derived BHMF is represented in Fig. 2 by the solid line surrounded by the grey area. The 'grey' area represent an error estimate on the BH mass function obtained by varying the parameters used in each of the above steps. The BHMF has $\rho_{\mathrm{BH}} = (5 \pm 2)\times10^5\mathrm{M}_\odot\,\mathrm{Mpc}^{-3}$ and this value is in agreement with $\rho_{\mathrm{BH}} = (3 \div 6)\times10^5\mathrm{M}_\odot\,\mathrm{Mpc}^{-3}$ obtained by Fabian & Iwasawa (1999) and Salucci et al. (1999) from the hard XRB.

The model results are shown in Fig. 2a. The solid line outside of the grey area is the BH mass function expected from type 1 AGNs only with a starting redshift of $z_\circ = 3$. The starting redshift at which we make the assumption that all Black Holes are active is not important for the final results. Indeed the dashed line representing the BHMF obtained assuming $z_\circ = 5$ is not significantly different from the one with $z_\circ = 3$. From the figure it is clear that Optical QSOs (high L AGNs) produce black holes with masses $M_{\mathrm{BH}} > 10^8$ $\mathrm{M}_\odot$ while X-ray AGNs (low L AGNs) produce the lower mass ones. Moreover, comparing the BHMF obtained from AGN activity at $z = 0$ with the one at $z_\circ$ it can be clearly seen that BH masses are produced during the AGN activity: this is the main reason why the results are little sensitive to the initial conditions. The model presented in the figure has R_{2-1}=0, i.e. it considers only unobscured AGNs, thus it is not unexpected that it does not account for the local BH mass function and the comparison between the 'observed' local BHMF with the one deduced from AGN activity yields a constraint on R_{2-1}. Let's first consider high L objects. It is found that $1 < \mathrm{R}_{2-1} < 2$ is required to match the local BHMF in absolute level (the slope at high mass is nicely reproduced). Correspondingly $\rho_{\mathrm{BH}} = 3.2 \div 4.6\times10^5 M_{\mathrm{BH}}$ Mpc^{-3}. Let's now focus on the low L AGNs. The existence of low L type 2 AGNs is well know and the local ratio is R_{2-1}=4. With that ratio,

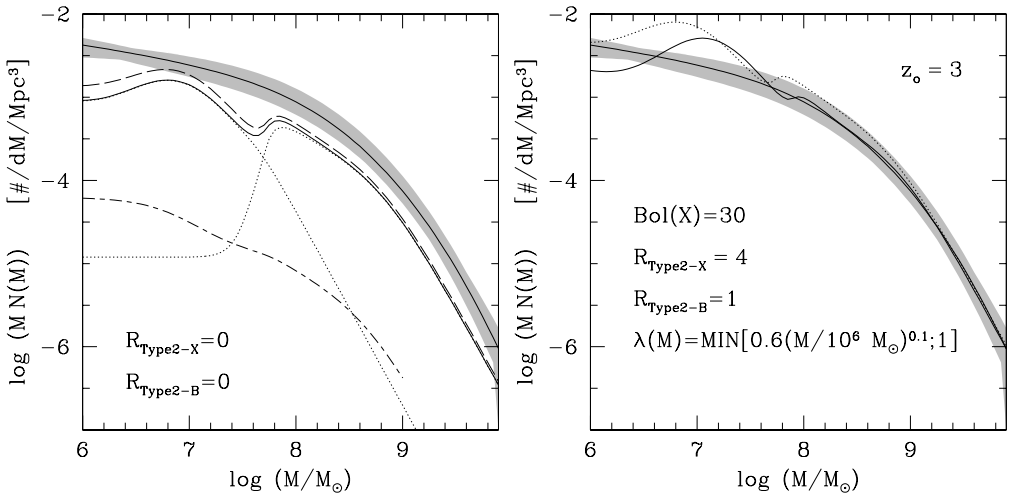

Fig. 2. Local BH mass function (left panel) from galaxy bulges (solid line in grey area) compared with BH mass function obtained considering only type 1 AGNs (solid line). The dotted lines are the contributions from low and high L AGNs. The dot-dashed line is the BH mass function at the redshift $z_\circ$=3 when all BHs were active. The dashed line represents the BHMF from AGN activity assuming that only 10% of the BHs were active at $z_\circ$=5. BHMFs from AGN activity (right panel) computed with $R_{2-1,X}$=4 and $R_{2-1,B}$=1, $L/L_X = 30$ and $L/\nu_B L\nu_B = 15$. In the model represented by the dotted line all AGNs are emitting at their Eddington luminosity, while with the solid line AGNs are emitting at a fraction of their Eddington luminosity which depends on M as specified in the figure.

the local BHMF at low masses ($M_{BH} < 10^8$ $M_\odot$) is overproduced (see Fig. 2b, dotted line). A change in the bolometric correction does not improve the situation because the BHMF is just shifted along the M axis. A possible solution to this problem is that low luminosity AGNs are not emitting at the Eddington Luminosity (see Fig. 2b, solid line), a possibility also considered in other works (e.g. Salucci et al. 1999 and references therein), and indeed, apart for some 'wiggles', the BHMF is now well reproduced. One must keep in mind that this might also mean that there are some problems with the AGN luminosity functions at low luminosities or that the M_{BH}-M_{Bulge} relation is different at low masses.

The main conclusion of this work is that with 'reasonable' assumptions, compatible with current knowledge, mass accretion onto massive BH during AGN activity can explain the local BH mass function both in shape and normalization. There is not much room for a large ($R >> 1$) population of high luminosity obscured AGNs (i.e. type 2 quasars).

6. The XMM bright serendipitous source sample (contributed by A. Caccianiga)

6.1. The sample

The XMM Bright Serendipitous Source Sample (XMM BSS) is part of the follow-up program being conducted by the XMM-Newton Survey Science Center (SSC)[1].

[1] The SSC is an international collaboration involving a consortium of several institutions, appointed by ESA, to exploit the

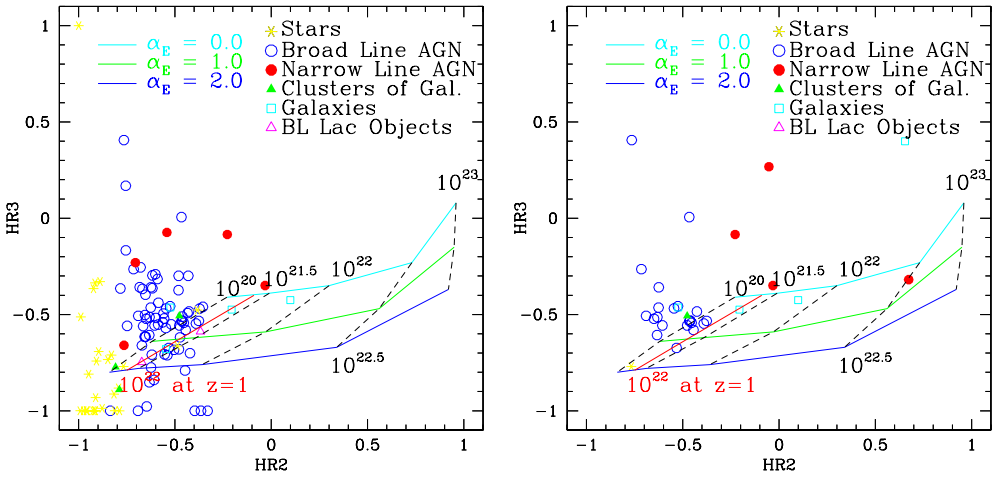

Fig. 3. HR2 vs. HR3 for the objects belonging to the XMM BSS 'soft' sample (left panel) and to the XMM BSS 'hard' sample (right panel). HR2 and HR3 for each source have been computed using the source count rate in the (0.5−2 keV), (2−4.5 keV) and (4.5−7.5 keV) energy band according to: $HR2 = \frac{C(2-4.5\,\mathrm{keV})-C(0.5-2\,\mathrm{keV})}{C(2-4.5\,\mathrm{keV})+C(0.5-2\,\mathrm{keV})}$ and $HR3 = \frac{C(4.5-7.5\,\mathrm{keV})-C(2-4.5\,\mathrm{keV})}{C(4.5-7.5\,\mathrm{keV})+C(2-4.5\,\mathrm{keV})}$. We have used different colors to mark the identified objects and, for clarity, we have not reported error bars. We have also reported the expected HR2 and HR3 values for an absorbed power-law model as a function of energy spectral index (α_E) and intrinsic absorbing column density (N_H). Note that many of the sources in the XMM BSS are outside the loci expected from a simple absorbed power-law suggesting more complicated models.

The XMM BSS is carried out at the Osservatorio Astronomico di Brera (Milan, Italy) and consists of two flux-limited samples having flux limit of $\sim 10^{-13}$ erg cm^{-2} s^{-1} in the 0.5–4.5 keV (XMM BSS 'soft' sample) and in the 4.5-7.5 keV (XMM BSS 'hard' sample) energy band. More details about the two samples are reported in Della Ceca et al. (2001).

As of today, 195 suitable XMM fields have been analyzed and a first sample of 331 sources selected: 321 sources belongs to the 'soft' sample and 64 sources to the 'hard' sample with 54 sources in common. The optical counterpart of the majority (85-90%) of these X-ray sources has an optical magnitude above the POSS II limit ($R \sim 21^{mag}$), thus allowing spectroscopic identification on a 4-m telescope. It is worth noting that, given the accuracy of the X-ray positions (2-5 arcsec at the 90% confidence level) and the magnitude of the expected optical counterpart, only one object needs to be observed to obtain the optical identification. For this reason the complete spectroscopic identification of the two samples is feasible with a reasonable number of telescope nights. Up to now 120 sources have been spectroscopically identified (either from the literature or from our own observations) leading to a 35% and 48% identification level for the 'soft' and 'hard' samples respectively.

XMM serendipitous detections for the benefit of the international scientific community (see `http://xmmssc-www.star.le.ac.uk` for a full description of the program).

6.2. First results

Although the identification level for the two XMM BSS samples is far from being complete, some general conclusions can be already drawn:

1) The hardness-ratio distribution. The majority of the X-ray sources have enough statistics (hundreds of counts) to allow X-ray studies in terms of energy distributions, source extent and flux variability. This fact allows us to investigate the overall properties of the sources in deeper detail than possible with fainter samples and to place this investigation on firm and solid statistical ground. A 'complete' spectral analysis for all the sources in the XMM BSS is in progress; in the meantime a 'snapshot' of the X-ray spectral properties of the sources obtained using the 'hardness ratio' method (equivalent to the 'color-color' analysis largely used at optical wavelengths) is shown in figure 1. A fairly sharp separation between different classes of sources is visible from figure 1: The HR2 value, in particular, discriminates between stars (HR2<-0.8), Broad Line AGNs ($-0.8<$HR2<-0.3) and Narrow Line AGNs (HR2>-0.3, except for some cases). Besides the theoretical implications of this segregation, the sensitivity of the HR2 value to the optical spectral type of the X-ray sources can offer a powerful tool to increase the efficiency for the selection of rare and interesting classes of objects (e.g. the absorbed AGNs).

2) The discovery of X-ray Bright Optically Normal Galaxies (XBONG). The existence of a population of galaxies posing as 'normal' elliptical galaxies in the optical band but showing strong signs of AGN activity in the X-ray band is an important topic hotly discussed in the recent literature (see also Sec. 4.1). Medium and deep surveys carried out with Chandra and XMM-Newton telescopes are discovering some examples of this intriguing class (e.g. Fiore et al. 2000; Barger et al. 2001; Comastri et al. 2002a). Unfortunately, in the majority of cases, a detailed analysis of the X-ray spectrum of these objects is not possible due to the weakness of the X-ray emission.

As expected, in the XMM BSS samples we are finding more examples of these galaxies. Unlike the other surveys, the XMM BSS is able to perform a detailed analysis of the X-ray spectra of these objects thanks to the relatively bright flux limit chosen to define the samples. A study of 4 galaxies discovered so far in the XMM BSS will be presented in Severgnini et al. (in preparation). The most important results can be summarized as follows:

(a) all the 4 objects contain a point-like (at the XMM resolution) AGN with $L_X = 10^{42}$ – 10^{44} erg s^{-1};
(b) the X-ray spectra show a great variety of AGN types, from absorbed ($N_H = 2 \times 10^{23}$ cm^{-2}) to unabsorbed AGNs;
(c) based on the results obtained from the X-ray analysis and by modeling the observed optical spectrum as the sum of different components (i.e. the host galaxy plus the absorbed or unabsorbed AGN) we find that the 'passive' appearance of the optical spectrum, in most cases, does not necessarily require the existence of a 'non-standard' AGN but can be easily explained as due to the combination of absorption/faintness of the AGN with respect to the host galaxy or with the presence of a BL Lac object.

7. The relationship between the BAL QSOs and the general population of AGN (contributed by P. Marziani and C. Bongardo)

Most unsolved issues in (unobscured) AGN research are ultimately reconcilable to the inability to unambiguously map observational parameters (like optical and UV emission line properties) into the physical parameter space of any accreting system, i.e., compact object mass M, Eddington ratio, and compact object spin. In the case of AGN, an aspect angle i (ideally the an-

gle between the line of sight and the accretion disk axis) is of special importance. It is also unclear how these parameters may relate 'unobscured' (Seyfert 1 nuclei, blazars and quasars) and 'obscured' AGN (Seyfert 2; mixed Starburst/AGN systems, BAL QSOs etc.) which have recently attracted so much attention and telescope time. Clearly, additional effects related to the environment are at play. Type 2 AGN – no matter their luminosity – seem to possess a circumgalactic environment systematically richer than the ones of type 1 host galaxies (e. g., Krongold et al. 2002), and statistically non different from the one of star-forming galaxies. Moreover, several heavily obscured systems belong to strongly interacting systems (e.g., Marziani et al. 2001, and references therein).

Broad Absorption Lines (BAL) QSOs occupy a special place among obscured AGN, since their continuum in the optical/UV range is not markedly different from that of other powerful quasars. The distinguishing features of BAL QSOs are deep absorption through in the UV and almost completely absent soft/hard X ray emission. Their nature in uncertain as far as frequency of occurrence, aspect parameter, and evolution are concerned. More explicitly, one can ask whether there is a luminosity threshold, or a critical Eddington ratio that makes BAL QSOs possible. Or, are BAL QSOs just 'every quasar's side-view?' Is there an evolutionary link between BAL QSOs and 'normal' QSOs?

At present, we can provide some preliminary answers to these questions, thanks to the correlations among the fundamental observational parameters that describe AGN diversity. The strongest emission line correlations are usually referred to as the 'Eigenvector 1' (E1) correlations. The name stems from a principal component analysis of the low redshift ($z \lesssim 0.5$) part of the Palomar-Green quasar sample (Boroson & Green 1992). For a number of reasons, we defined an optical E1 in terms of two main parameters: FWHM(Hβ), and the equivalent width ratio of the Fe II emission (the λ4570 blend measured between 4430 and 4600 Å) and Hβ (Sulentic et al. 2000).

To take advantage of the E1 correlations, we screened several spectral databases for UV absorptions. It was possible to define a sample of 12 BAL QSOs within the limits of absorption W(C IVλ1549) $\gtrsim$4 Å, $z \lesssim 0.5$, and $m \lesssim$ 16.0. Six of the 12 objects have a Balnicity Index $\gtrsim$0 (Weymann et al. 1991). The remaining six can be considered as so-called 'mini-BAL' QSOs (i.e., quasars with *bona fide* broad absorption that do not meet the restrictive BALnicity criterion). Unlike their high-z brethren, low-z BAL QSOs have easily obtainable E1 parameters.

Two BAL QSOs with BALnicity $\gtrsim$0 fall in the region believed to represent higher Eddington ratio ($\propto$ L/M) and larger i. Three lie significantly above the sequence where most AGN are located (interestingly, they are the *only* outliers). The spectral energy distribution of these 3 outliers (PG 0043+039, Mkn 231, IRAS 07598+6508) is markedly different from the one of the other BAL QSOs in the far IR, with a prominent excess which points towards a composite Starburst/AGN nature. The Hβ profile of the outliers shows an additional blueshifted component. If a correction is applied, the data point for IRAS 07598+6508 moves into the area of very high L/M and large i. Similar considerations can be applied to the remaining two sources. The high terminal velocity of the six BAL QSOs (20000–30000 km s^{-1}) also suggest large value of L/M if a radiation pressure driven wind is at the origin of the outflow. The lack of detection in ASCA spectra of three of the six sources is consistent with a photon index $\Gamma \approx 3$ (as observed among 'Narrow-Line' Seyfert 1 sources), since, for-non-detection, this would require $N_H \gtrsim 5 \times 10^{22}$ cm^{-2}, above the minimum N_H requirement for UV absorptions. We infer that radio-quiet BAL QSOs are preferentially objects radiating at large Eddington ratio. This condition seems, at least in the outlying sources (and perhaps even in all BAL BQSO we considered), coeval with heavy obscuration and

with a surrounding Starburst (Marziani et al. 2002, in preparation).

Much work remains to be done. We collected Hβ observations for more BAL QSOs in the range $0.5 \lesssim z \lesssim 0.8$. Several $z \gtrsim 0.9$ quasars were observed with VLT/ISAAC. The circumgalactic environment and morphology of BAL QSOs hosts should be thoroughly investigated. Yet, the fundamental question remains why BAL QSOs are so rare at low luminosity, even if L/M is expected to be high. A promising strategy could be to investigate any dependence of the outflow opening angle on luminosity.

8. XMM Observations of ULIRGs
(contributed by V. Braito)

Luminous Infrared Galaxies (hereafter ULIRGs) are an enigmatic class of sources with luminosities in excess to 10^{12} $L_{\odot}$ (i.e. comparable to QSO luminosities) which emit most of their energy in the far-IR (FIR) domain. It is widely accepted that both Starburst and AGN activity should be responsible for the observed emission but their relative contribution is still unconstrained and, in some cases, the presence of an AGN is unclear. Hard X-ray ($E > 2$ keV) observations, less affected by photoelectric absorption, offer an additional important tool to investigate the presence of hidden AGNs, and to obtain quantitative estimates of their contribution to the bolometric luminosity. We are carrying out a mini-survey with XMM-Newton of 10 nearby ULIRGs, selected from the Genzel sample (Genzel et al. 1998), which is flux-limited at 60 μm and complete to $S_{60} \geq 5.4$ Jy. Our purpose is not only to identify AGN signatures in hard X-rays, but also to quantify the separate contributions of buried AGN and Starburst emissions and to estimate their relative contribution to the high observed FIR emission. Eight of the ULIRGs have been already observed with XMM. All the sources are clearly characterized by a soft ($E \lesssim 2$ keV) X-ray emission which can be modeled with thermal emission (produced in the Starburst region) with $kT \sim 0.7$ keV. However, this model can in no case account for the extra emission at energy above few keV. For IRAS 19254-7245, IRAS 20551-4250 and Mkn 231 clear signatures of AGN activity are present in the X-ray spectra. IRAS 20551-4250 is an example of ULIRG which, classified as a pure Starburst from optical and IR spectroscopy, clearly hosts an obscured AGN. For IRAS 19254-7245 we have detected, for the first time, a strong (EW $\sim$ 2.0 keV) emission line at ~ 6.49 keV (rest-frame) which, along with the hard continuum emission, is highly indicative of a Compton-thick source. For Mkn 231 our data confirm the presence of a flat spectrum ($\Gamma = 1.1$) and only a marginally detected, moderately intense, Fe line (EW$\sim$200 eV). For the remaining 5 sources already observed, the data statistics does not allow us to reach definitive conclusion on the nature of the hard X-ray emission, albeit the presence of a buried AGN remains a possibility.

References

Akiyama, M., et al. 2000, ApJ, 532, 700
Alexander, D., et al. 2001, ApJ, 554, 18
Antonucci, R. 1993, ARA&A, 31, 473
Baldi, A., Molendi, S., Comastri, A., Fiore, F., Matt, G., & Vignali, C. 2002, ApJ, 564, 190
Barger, A., Cowie, L., Mushotzky, R. F., & Richards, E. A. 2001, AJ, 121, 662
Barger, A., Cowie, L., Brandt, W. N., Capak, P., Garnire, G. P., Hornschemeier, A. E., Steffen, A. T., & Wehner, E. H. 2002, AJ, 124, 1834
Bianchi, S., Matt, G., & Iwasawa, K. 2001, MNRAS, 322, 669
Boroson, T. A., & Green, R. F. 1992, ApJS, 80, 109
Boyle, B. J., et al. 2000, MNRAS, 317, 1014
Brandt, W. N., et al. 2001, AJ, 122, 2810
Cagnoni, I., della Ceca, R., & Maccacaro, T. 1998, ApJ, 493, 54
Comastri, A. 2001, in X-ray Astronomy '99: Stellar Endpoints, AGNs and the Diffuse X-ray Background, ed. N. E. White, G.

Malaguti, & G. C. Palumbo (New York: AIR), AIP Conf. Ser. 599, 73
Comastri, A., et al. 2002a, ApJ, 571, 771
Comastri, A., et al. 2002b, in New Visions of the X–ray Universe in the XMM–Newton and Chandra Era, ed. F. Jansen, ESA SP–488, 267
Della Ceca, R., et al., 2001, in Proc. ESTEC, The Netherlands
Fabbiano, G., Kim, D. W., & Trinchieri, G. 1992, ApJS, 80, 531
Fabian, A. C., & Iwasawa, K. 1999, MNRAS, 303, L34
Fiore, F., et al. 2000, NewA, 5, 143
Fiore, F., et al. 2001, MNRAS, 327, 771
Genzel, R., et al. 1998, ApJ, 498, 579
Giacconi, R., et al. 2002, ApJS, 139, 369
Gilli, R., Salvati, M., & Hasinger, G. 2001, A&A, 366, 407
Granato, G. L., Danese, L., & Franceschini, A. 1997, ApJ, 486, 147
Gruppioni, C., et al. 2002, MNRAS, 335, 831
Guainazzi, M., et al. 1998, MNRAS, 301, L1
Hasinger, G., et al. 2001, A&A, 365, L45
Kinkhabwala, A., et al. 2002, ApJ, 575, 732
Krongold, Y., et al. 2002, ApJ, 572, 169
Lari, C., et al. 2001, MNRAS, 325, 1173
Lehmann, I., et al. 2001, A&A, 371, 833
Mainieri, V. et al. 2002, A&A, 393, 425
Marconi, A., & Salvati, M. 2002, in Issues in Unification of Active Galactic Nuclei, ed. R. Maiolino, A. Marconi, & N. Nagar (San Francisco: ASP), ASP Conf. Ser. 258, 217
Marziani, P., et al. 2001, The Central Kiloparsec of Starbursts and AGN: The La Palma Connection ed. J. H. Knapen, et al. (San Francisco: ASP), ASP Conf. Ser. 249, 284
Maiolino, R., & Rieke, G. H. 1995, ApJ, 454, 95
Matt, G. 2000, A&A, 355, L13
Matt, G., 2002, RSPTA, 360, 2045
Matt, G., et al. 2000, MNRAS, 318, 173
Matt, G., Guainazzi, M., & Maiolino, R., 2003, MNRAS, submitted
Matute, I., et al. 2002, MNRAS, 332, L11
Oliver, S., et al. 2000, MNRAS, 316, 749
Risaliti, G., Maiolino, R., & Salvati, M. 1999, ApJ, 522, 157
Salucci, P., et al. 1999, MNRAS, 307, 637
Sambruna, R., et al. 2001, ApJ, 546, L9
Small, T. A., & Blandford, R. D. 1992, MNRAS, 259, 725
Sulentic, J. W., Marziani, P. & Dultzin-Hacyan, D. 2000, ARA&A 38, 521
Weymann, R., et al. 1991, ApJ, 373, 23